Controls of temperature and mineral growth rate on lithium and sodium incorporation in abiotic aragonite

Jean-Michel Brazier, Anna Harrison, Claire Rollion-Bard, Vasileios Mavromatis

Chemical Geology 654 (2024) 122057

Contents lists available at ScienceDirect

Chemical Geology

journal homepage: www.elsevier.com/locate/chemgeo

Controls of temperature and mineral growth rate on lithium and sodium incorporation in abiotic aragonite

Jean-Michel Brazier [a,*,1], Anna L. Harrison [b,1], Claire Rollion-Bard [c], Vasileios Mavromatis [b,1]

[a] Institute of Applied Geosciences, Graz University of Technology, Rechbauerstrasse 12, 8010 Graz, Austria
[b] Geosciences Environnement Toulouse (GET), Observatoire Midi-Pyrénées, Université de Toulouse, CNRS, IRD, UPS, 14 Avenue Edouard Belin, 31400 Toulouse, France
[c] Laboratoire des Sciences du Climat et de l'Environnement/IPSL, CEA-CNRS-UVSQ, Gif sur Yvette, France

ARTICLE INFO

Editor: Dr. Hailiang Dong

Keywords:
Lithium
Sodium
Aragonite
Distribution coefficient
Growth rate
Temperature
Li/Mg

ABSTRACT

The use of Li/Ca, Na/Ca and Li/Mg ratios in biogenic aragonite exhibits high potential for reconstructing environmental parameters such as temperature and/or salinity. To date however, only a little is known about the mechanisms controlling the incorporation of monovalent metals such as Li^+ and Na^+ in aragonite. In this study, the effects of temperature and growth rate on Li and Na incorporation into abiotically precipitated aragonite were experimentally investigated. The results for aragonite overgrowths at 5, 15 and 25 °C and for the surface normalized growth rate range $10^{-8.6} \leq r_p \leq 10^{-7.1}$ (mol/m^2/s) suggest that apparent distribution coefficients (i.e., $D_{Me^+} = \frac{\left(\frac{C_{Me^+}}{C_{Ca}}\right)_{aragonite}}{\left(\frac{m_{Me^+}}{m_{Ca}}\right)_{solution}}$) of Li and Na are mainly controlled by mineral growth rate, whereas temperature has a minor effect. The combined effect of growth rate and temperature on D_{Li} and D_{Na} can be described as:

$$Log\ D_{Li} = 0.836(\pm 0.028)\ Log\ r_p - 0.026(\pm 0.002)\ T + 2.958(\pm 0.221); R^2 = 0.97$$

$$Log\ D_{Na} = 0.456(\pm 0.030)\ Log\ r_p - 0.018(\pm 0.002)\ T - 0.253(\pm 0.234); R^2 = 0.90$$

where Log r_p is the growth rate in mol/m^2/s and T is the temperature in degrees Celsius.

The D_{Li} and D_{Na} values increase at increasing mineral growth rate, but also decrease as a function of temperature in experiments with similar normalized growth rate. These observations suggest that the incorporation of Li and Na in abiotic aragonite is controlled by the density of mineral surface defect sites that are correlated with the degree of saturation of the reactive solution with respect to aragonite. Interestingly, no correlation between Li/Mg in the aragonite overgrowths and temperature of formation was observed in this study. This difference of Li/Mg and temperature correlations between abiotic aragonite and natural biogenic samples is intriguing and underlines the need for robust understanding of elemental incorporation during carbonate mineral formation, and proxy calibrations specific for growth conditions (e.g., abiotic versus biogenic). The results of this study do not support the use of Li/Mg as a temperature proxy in abiotic aragonite.

1. Introduction

The trace element content and ratios in carbonate minerals are routinely used for the reconstruction of paleoenvironmental and paleoclimatic conditions that occurred at the time of mineral formation. In this context, the mechanisms controlling the elemental compositions of carbonate minerals have been extensively studied over the past 50 years (e.g., Lorens, 1981; Mucci and Morse, 1983; Dromgoole and Walter, 1990; Morse and Bender, 1990; Paquette and Reeder, 1995; Temmam et al., 2000; Gabitov and Watson, 2006; Gaetani and Cohen, 2006; Lakshtanov and Stipp, 2007; Gabitov et al., 2008; Tang et al., 2008; Mavromatis et al., 2013, 2017; Goetschl et al., 2019; Gabitov et al.,

* Corresponding author.
E-mail address: jean-michel.brazier@unibe.ch (J.-M. Brazier).
[1] Current address: University of Bern, Institute of Geological Sciences, Baltzerstrasse 1 + 3, 3012 Bern, Switzerland

https://doi.org/10.1016/j.chemgeo.2024.122057
Received 23 January 2024; Received in revised form 19 March 2024; Accepted 20 March 2024
Available online 21 March 2024

2021; Brazier and Mavromatis, 2022; Brazier et al., 2023). Most of these earlier works have focused on the incorporation of divalent cations (i.e., Me^{2+}) in $CaCO_3$ minerals and assume an ideal substitution between Ca^{2+} and Me^{2+} that leads to the formation of a diluted solid solution (e.g., Reeder et al., 1999; Finch and Allison, 2007, 2008). Note here that the substitution process may require a change of the bonding environment of the trace metal in the mineral structure compared to the end-member pure phase. For example, the presence of Ba in calcite reduces its coordination to six (Reeder et al., 1999), whereas it coordinates to nine oxygens in the pure Ba carbonate mineral phase, witherite (Finch et al., 2010). Although the presence of Me^{2+} in $CaCO_3$ minerals can be modelled as an ideal replacement for Ca^{2+} in the solid, the mechanisms controlling the presence of other traces in carbonate minerals such as monovalent (i.e., Me^{+}) or trivalent cations (e.g. REE) cannot be approached with the same ideal replacement assumption. For example, the presence of trivalent REEs in calcite has been explained by several models including the simultaneous incorporation of Na^{+} or the presence of a vacancy in the solid (e.g., Zhong and Mucci, 1995; Lakshtanov and Stipp, 2004; Voigt et al., 2017).

Earlier works studied the incorporation of Me^{+} into calcite and aragonite (White, 1977; Busenberg and Plummer, 1985; Okumura and Kitano, 1986; Marriott et al., 2004a; Yoshimura et al., 2017; Füger et al., 2019), with several models proposed to explain the mechanisms of Me^{+} incorporation in carbonate minerals. Notably, incorporation at interstitial sites (White, 1977; Okumura and Kitano, 1986), double substitution for Ca^{2+} compensated by the incorporation of SO_4^{2-} or altervalent substitution for Ca^{2+} compensated by vacancies of CO_3^{2-} have been suggested (White, 1977; Yoshimura et al., 2017). More recently, based on the variations of Li and Na concentration in calcite as a function of pH in experiments performed under similar surface normalized growth rates, Füger et al. (2019) suggested the formation of $>NaHCO_3^0$ or $>LiHCO_3^0$ and their further incorporation in the solid. The same group of authors, however, in a more recent study using δ^7Li composition of the precipitated calcite suggested that more than one species or bonding environments in the solid can explain variations of δ^7Li as a function of pH (Füger et al., 2022).

Although a robust mechanistic model describing the incorporation of Me^{+} in carbonate minerals does not exist at present, Li and Na are of great interest for the geoscientific community because empirical observations in natural samples have shown that their elemental ratios with other elements (e.g., Li/Ca, Na/Ca, Li/Mg) in biogenic carbonate minerals (e.g., corals, foraminifera) can be used to reconstruct physicochemical parameters including the degree of saturation of the solution with respect to $CaCO_3$ minerals, the temperature, the salinity, the pH, or the growth rate (Hall and Chan, 2004; Marriott et al., 2004a; Lear and Rosenthal, 2006; Lear et al., 2010; Bryan and Marchitto, 2008; Montero-Serrano et al., 2013; Raddatz et al., 2013; Wit et al., 2013; Montagna et al., 2014; Rollion-Bard and Blamart, 2015; Fowell et al., 2016, Bonneau et al., 2018; Cuny-Guirriec et al., 2019; Stewart et al., 2020). These earlier works provide species-specific elemental correlation for biogenic carbonates, however, to date, only a few studies have investigated the mechanisms controlling the incorporation of Li and Na into abiotic carbonate minerals under strictly controlled conditions. Among them, the two studies by Marriott et al. (2004a, 2004b) showed that the incorporation of Li into calcite is temperature and salinity dependent. More recently, Füger et al. (2019) have shown that the incorporation of Li into calcite is strongly dependent on the growth rate, but also on the pH of the reactive solution. Considering that biogenic carbonates commonly consist of aragonite (e.g. corals), it is also worth exploring the parameters controlling Li and Na incorporation into abiotic aragonite, as this may also provide valuable insights regarding the controls of elemental distribution in abiotic and biogenic aragonite.

The goal of this study is to quantify the effect of mineral growth rate and temperature on the incorporation of Li and Na in aragonite. Overgrowth experiments on aragonite seeds were performed at three temperatures (5, 15 and 25 °C) following the constant addition method (Mavromatis et al., 2022). These experiments allow quantification of the distribution coefficient for Li and Na between aragonite and fluid as well as the dependence of the D_{Me} on temperature and growth rate. The results also provide insight into the dependence of the Na/Mg and Li/Mg ratios in aragonite on temperature and growth rate.

2. Methods

2.1. Overgrowth experiments

The experimental solids and fluids used in this study (Fig. 1) have been produced in the work by Mavromatis et al. (2022), which reported the distribution coefficients of Mg during abiotic aragonite growth (see Table 1). Overgrowth experiments were conducted in a thermostatic cabinet at 5, 15 and 25 °C in the presence of Li, Mg, and Na using the constant addition technique (Tesoriero and Pankow, 1996; Mavromatis et al., 2013, 2015; Voigt et al., 2017). This setup allows for carbonate mineral growth under chemical steady-state conditions and enables robust estimations of mineral growth rate and distribution coefficients. In the experimental runs, aragonite growth occurred in a reactive solution containing ~270 mM NaCl, ~25 mM $MgCl_2$ and ~ 10 mM LiCl. Mineral growth on aragonite seeds was induced by the continuous addition of two inlet solutions with the first containing $CaCl_2$ together with $MgCl_2$ and LiCl, and the second containing Na_2CO_3. Aragonite growth rate was varied by changing the concentrations of $CaCl_2$ and Na_2CO_3 between 40 and 240 mM in the inlet solution and their addition rates by peristaltic pump (see Table A.1). The pH and alkalinity in these reactors were kept constant within a run by the continuous bubbling of humidified laboratory air through the reactive solution. The reactors contained initially 500 mL of solution and were equipped with a Teflon-coated floating stir bar rotating at 240 rpm (rotation per minute). The stirring was stopped prior to sampling of the reactive solution (every 12 or 24 h) to let the aragonite settle, leading to a variation of the solid/solution ratio within a maximum of ±4%. Immediately after sampling, the solutions were filtered through 0.2 μm cellulose acetate syringe filters and stored in a fridge at ~4 °C. At the end of the experimental runs, the entirety of the reactive solution was vacuum filtered through a 0.2 μm cellulose acetate filter and the solids were rinsed with deionized water and dried at 40 °C.

2.2. Fluid and solid analyses

The alkalinity of fluid samples was measured by HCl titration using an automatic Schott TitroLine alpha plus titrator with an uncertainty of ±2%. The pH was measured using a SenTix® 945 pH gel electrode from WTW, calibrated against NIST standard buffers. The recorded pH values

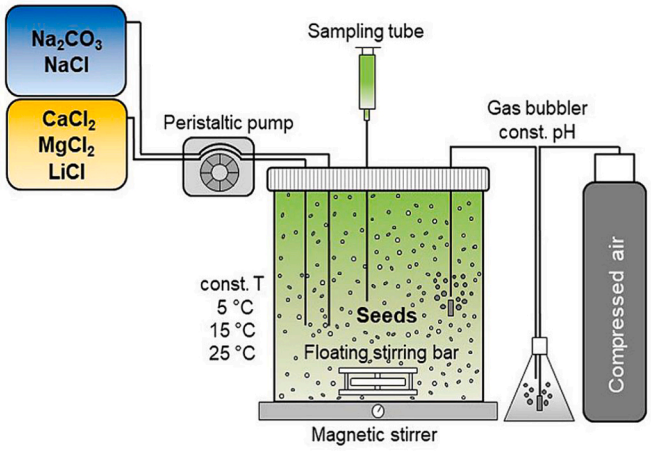

Fig. 1. Experimental setup. Const. = constant.

Table 1
Temperature, average pH and alkalinity (in mmol/L) of the reactive solution at steady state (pH_{ss} and $Alk._{ss}$, respectively), saturation indices of the solutions with respect to aragonite ($SI_{aragonite}$), aragonite growth rate (Log r_p in mol/m^2/s), Li/Ca (in mmol/mol), Na/Ca (in mmol/mol), Li/Mg (in mol/mol), and Na/Mg (in mol/mol) ratios in aragonite overgrowth, and distribution coefficients of Li, Na, and Mg in aragonite (Mg values are from Mavromatis et al., 2022).

Experiment	Temperature (°C)	pH_{ss}	$Alk._{ss}$ (mmol/L)	$SI_{aragonite}$	Log r_p (mol/m^2/s)	aragonite overgrowth				Log D_{Li}	Log D_{Na}	Log D_{Mg}
						Li/Ca (mmol/mol)	Na/Ca (mmol/mol)	Li/Mg (mol/mol)	Na/Mg (mol/mol)			
LiAr-1	25	8.09	1.35	0.05	−8.6	0.04	2.03	0.30	15.58	−4.95	−4.62	−4.77
LiAr-2	25	8.14	1.37	0.10	−8.2	0.08	3.39	0.39	16.62	−4.57	−4.37	−4.55
LiAr-3	25	8.19	1.43	0.16	−7.9	0.14	3.31	0.51	11.88	−4.33	−4.38	−4.52
LiAr-4	25	8.2	1.46	0.27	−7.6	0.19	3.30	0.64	10.96	−4.11	−4.30	−4.43
LiAr-5	25	8.27	1.72	0.41	−7.5	0.36	3.74	0.99	10.35	−3.82	−4.22	−4.19
LiAr-6	25	8.3	1.72	0.43	−7.5	0.33	3.88	1.03	11.92	−3.86	−4.21	−4.25
LiAr-13	25	8.17	1.95	0.10	−8.3	0.05	2.82	0.36	19.65	−4.75	−4.48	−4.70
LiAr-14	25	8.24	2.15	0.23	−7.9	0.16	5.36	0.62	20.97	−4.25	−4.18	−4.43
LiAr-15	25	8.36	2.77	0.43	−7.4	0.36	6.47	0.68	12.16	−3.91	−4.12	−4.13
LiAr-16	25	8.39	3.07	0.60	−7.1	0.46	7.29	0.67	10.63	−3.68	−3.94	−3.90
LiAr-17	25	8.4	2.72	0.59	−7.1	0.47	7.25	0.69	10.74	−3.64	−3.91	−3.86
LiAr-18	25	8.39	2.52	0.60	−7.1	0.43	6.59	0.72	10.93	−3.65	−3.92	−3.89
LiAr-39	25	8.08	2.26	0.28	−7.8	0.13	2.17	0.61	10.09	−4.16	−4.37	−4.33
LiAr-40	25	8.13	2.92	0.44	−7.7	0.23	3.61	0.77	12.16	−3.95	−4.18	−4.21
LiAr-42	25	8.2	3.18	0.58	−7.4	0.28	4.53	0.74	11.97	−3.80	−4.01	−4.08
LiAr-7	15	8.15	2.46	0.09	−8.6	0.07	2.05	0.41	12.59	−4.64	−4.59	−4.60
LiAr-8	15	8.21	2.55	0.17	−8.2	0.12	5.56	0.36	16.11	−4.36	−4.14	−4.27
LiAr-9	15	8.26	3.02	0.34	−7.9	0.27	6.29	0.62	14.52	−3.96	−4.04	−4.11
LiAr-10	15	8.29	3.12	0.45	−7.7	0.42	7.14	0.73	12.56	−3.70	−3.90	−3.86
LiAr-11	15	8.34	3.39	0.56	−7.4	0.51	7.92	0.63	9.72	−3.60	−3.84	−3.82
LiAr-12	15	8.36	3.43	0.58	−7.4	0.49	7.66	0.78	12.31	−3.61	−3.85	−3.91
LiAr-31	15	8.09	2.48	0.03	−8.3	0.10	2.95	0.38	11.48	−4.45	−4.42	−4.40
LiAr-32	15	8.21	2.79	0.23	−7.9	0.25	3.68	0.62	9.22	−4.02	−4.30	−4.19
LiAr-33	15	8.27	3.56	0.43	−7.4	0.53	7.12	0.64	8.70	−3.64	−3.96	−3.83
LiAr-34	15	8.32	3.43	0.52	−7.2	0.57	7.64	0.71	9.52	−3.55	−3.88	−3.77
LiAr-35	15	8.35	3.55	0.56	−7.1	0.57	7.60	0.74	9.97	−3.52	−3.84	−3.75
LiAr-36	15	8.43	3.57	0.67	−7.1	0.72	8.98	0.74	9.28	−3.40	−3.76	−3.64
LiAr-19	5	8.34	4.29	0.11	−8.6	0.18	7.88	0.30	12.94	−4.40	−4.22	−4.26
LiAr-20	5	8.37	4.90	0.23	−8.2	0.38	6.86	0.47	8.45	−4.05	−4.24	−4.10
LiAr-21	5	8.4	5.07	0.38	−7.9	0.72	9.90	0.69	9.48	−3.66	−3.97	−3.88
LiAr-22	5	8.41	4.79	0.47	−7.7	0.72	9.87	0.77	10.58	−3.60	−3.91	−3.87
LiAr-23	5	8.43	5.76	0.56	−7.6	0.86	11.02	0.72	9.14	−3.48	−3.83	−3.72
LiAr-24	5	8.48	5.86	0.66	−7.6	0.88	11.37	0.74	9.51	−3.41	−3.76	−3.66
LiAr-25	5	8.09	3.38	0.06	−8.3	0.09	7.00	0.35	26.10	−4.15	−4.00	−4.09
LiAr-26	5	8.16	3.87	0.23	−7.9	0.20	6.66	0.44	14.84	−3.79	−3.98	−3.97
LiAr-27	5	8.3	5.08	0.54	−7.4	0.53	10.31	0.68	13.07	−3.30	−3.71	−3.52
LiAr-28	5	8.35	5.50	0.63	−7.2	0.58	11.19	0.66	12.80	−3.26	−3.68	−3.38
LiAr-29	5	8.31	4.88	0.65	−7.1	0.87	10.90	0.82	10.20	−3.22	−3.57	−3.51
LiAr-30	5	8.36	5.63	0.72	−7.2	0.98	11.93	0.67	8.10	−3.18	−3.55	−3.38

have an uncertainty of ±0.05. Sodium concentrations in the fluid phase were measured using a Perkin Elmer Optima 8300 DV inductively coupled plasma optical emission spectrometer (ICP-OES) with an analytical precision of <±3% (RSD). The concentrations of Ca, Mg and Li were measured with an Agilent 7500CX Inductively Coupled Plasma Mass Spectrometer (ICP-MS) with an analytical precision better than 3% (RSD) based on repeated measurements of the samples in different measurement sessions. For each analytical session, the calibration standards were matrix-matched with the samples analyzed. A normalization to Sc, Se or Ge internal standards was used to correct the instrumental drift, and the accuracy of the measurements was ensured by repeated measurements of SPS-SW1 reference material, XXI standard solution from Merck, and in-house artificial solutions with adapted concentration to the considered samples. Aqueous speciation, ion activities and saturation states of the reactive solutions with respect to aragonite were calculated using PHREEQC Version 3 software together with its MINTEQ.V4 database (Parkhurst and Appelo, 2013) after the addition of the solubility products of hydromagnesite (Gautier et al., 2014) and nesquehonite (Harrison et al., 2019).

The mineralogy of the solids was confirmed by X-ray powder diffraction (XRD) analysis using a PANalytical X'Pert PRO diffractometer and Co-Kα-radiation (40 mA, 40 kV) in the 2θ range from 4° to 85° and with scan speed of 0.03°s^{-1}. The post-experimental qualitative characterization of the seed and solids was performed on the PANalytical HighScore Plus software together with the ICSD database and the mineral phases were quantified by Rietveld refinement with a precision better than 1 wt% and a detection limit of ~0.5 wt%. The solids were gold-coated and imaged on a ZEISS DSM 982 Gemini scanning electron microscope (SEM) equipped with a field emission gun operating at 5 kV accelerating voltage. The chemical composition of the solid phases was determined after their digestion with concentrated double distilled HNO_3 on an Agilent 7500CX Inductively Coupled Plasma Mass Spectrometer (ICP-MS) with an analytical precision better than 3% (RSD) using the same procedure described for the fluids above. All the precipitated solids were digested at least three different times, and each of these batches of digestion were measured at least three times. The seed material was digested five different times and the concentrations of the trace elements (i.e., Na and Li) were measured at least three times on each batch of digestion. The seeds contained 66 mmol/mol of Na but Li contents of the seeds was below detection limits. Finally, the specific surface areas of the solid samples before and after the experimental runs were determined by 11-point krypton adsorption BET method (Brunauer et al., 1938) using a Micromeritics Tristar II plus surface area analyzer.

3. Results

3.1. Chemical composition of the reactive solutions

An example of the temporal evolution of Ca, Mg and Li concentrations in the reactive solution, as well as the Li/Mg molar ratio can be seen in Fig. 2 for experiment LiAr-9 (Table 1). This illustrates that chemical steady-state conditions of the reactive solution with respect to aqueous Ca, Mg, Na and Li concentrations occur from the onset of the experimental runs. Under these chemical steady-state conditions, the growth rate of aragonite (i.e., r_p) is estimated based on mass balance considerations. Owing to the small variation in volume of the reactive solution per time unit (i.e., <4%) the amount of aragonite precipitated can be approximated by the moles of Ca introduced in ($n_{Ca(add)}$), corrected for the moles of Ca removed from the reactor during sampling ($n_{Ca(rem)}$) per time unit as:

$$r_p = \frac{\frac{n_{Ca(add)} - n_{Ca(rem)}}{86{,}400}}{S} \quad (1)$$

where S is the reactive surface of aragonite in m^2 and 86,400 is the number of seconds in 24 h. In Eq. (1) r_p is expressed in mol/m^2/s. Note here that Eq. (1) does not consider the presence of trace elements (i.e., Li, Mg, Na) in the solid phase because their concentrations do not exceed 0.98, 1.5 and 12 mmol/mol for Li, Mg and Na, respectively. The aragonite growth rate for the experiments conducted in this study ranges from $10^{\text{ to } 8.6}$ to $10^{-7.1}$ mol/m^2/s (Table 1).

3.2. Composition of the precipitated solids

The X-ray diffraction patterns of the precipitates collected at the end of the experimental runs are identical to those of the seed material. In all cases, the aragonite proportion is >98 wt% (with <2% of calcite coming from the seeds). All the solids exhibit a needle-like structure characteristic of aragonite (Fig. 3A-D). Surface features such as increased surface roughness, presence of steps or surface porosity can be seen on all the solids recovered at the end of experiments and are indicative of aragonite overgrowth on the seed material (Fig. 3B-D).

The concentration of Li in the aragonite overgrowths can be seen in Table 1 and achieved minimum values of 38.8, 66.5 and 93.1 µmol/mol for experiments performed at 25, 15 and 5 °C, respectively, whereas the maximum Li concentrations in aragonite overgrowth for the same temperatures were 469, 715 and 982 µmol/mol, respectively. Similarly, the minimum concentrations of Na in aragonite were 2.03, 2.05 and 6.66 mmol/mol for experiments performed at 25, 15 and 5 °C, respectively, whereas the maximum Na concentrations were 7.29, 8.98 and 11.9 mmol/mol, respectively (see Table 1). Note that the Na concentrations reported in Table 1 have been corrected for the Na present in the seeds. These results suggest that both Li and Na concentrations in the precipitated aragonite increase at decreasing temperature.

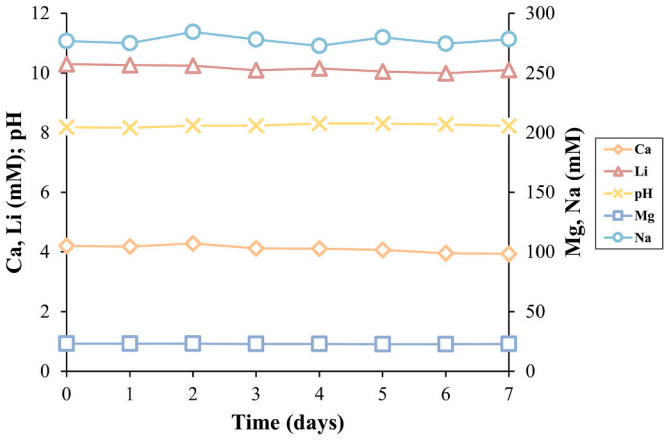

Fig. 2. Temporal evolution of Ca, Li, Mg concentrations, and pH of the fluid as a function of time for experiment LiAr-9.

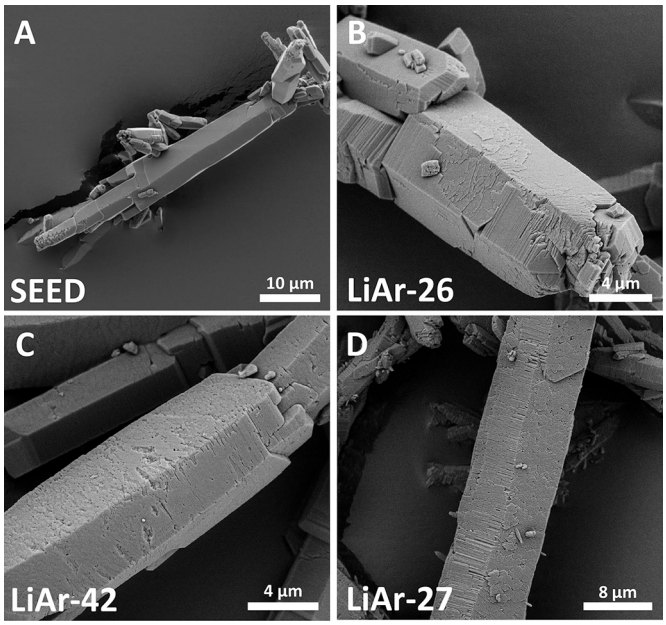

Fig. 3. Scanning electron microscope (SEM) images of (A) aragonite seed, overgrowth aragonite from (B) experiment LiAr-26, (C) experiment LiAr-42, and (D) experiment LiAr-27.

3.3. Lithium and sodium distribution between aragonite and the reactive solution

The incorporation of monovalent ions in aragonite cannot be modelled as a one-to-one replacement of Ca. As was summarized by Füger et al. (2019) the major hindrance for estimation of the distribution coefficient calculation arises from the charge imbalance due to the presence of Me^+ in the crystal lattice of a carbonate mineral. This means the distribution coefficient expressed as a ratio of trace-to-major ion does not imply a 1:1 substitution, unlike that originally envisaged in the Henderson-Kracek approach (Henderson and Kracek, 1927). In this study, we follow the nomenclature proposed earlier for the incorporation of monovalent ions in carbonate minerals (e.g., Ishikawa and Ichikuni, 1984; Marriott et al., 2004b) and we report apparent distribution coefficient of Li in aragonite as:

$$D_{Me^+} = \frac{\left(\frac{c_{Me^+}}{c_{Ca}}\right)_{aragonite}}{\left(\frac{m_{Me^+}}{m_{Ca}}\right)_{solution}} \quad (2)$$

where c stands for the concentrations of the metal in the solid phase (mol/mol $CaCO_3$) and m denotes the total molar concentration of the metal in the reactive solution. Considering that the moles of Li and Na in the precipitated aragonite are significantly lower than those of Ca, the parameter c_{Ca} can be considered equal to unity in Eq. (2).

In all the data reported, D_{Me^+} has been estimated using Eq. (2). Note here that the calculation of distribution coefficients is based on the use of the activities of the free aqueous ions which according to the classical mineral growth model (Burton et al., 1951) are the only species incorporated in the growing mineral phase. However, in this present study, Eq. (2) instead uses the total concentrations of the cations rather than their activities. This choice was made because complexation would affect the distribution of Ca to a greater extent than that of Li which generally does not form complexes in an aqueous solution (e.g., Füger

et al., 2019). Sodium does form aqueous complexes with anions such as (HCO_3^- and CO_3^{2-}), but the Na-DIC complexes are weaker compared to those of Ca^{2+} and represent a negligible amount of Na under the utilized experimental conditions (<0.4% of total aqueous Na is complexed).

The estimated values of D_{Li} and D_{Na} in all experimental runs can be found in Table 1. The minimum D_{Li} values at 25, 15 and 5 °C were 1.13×10^{-5}, 2.32×10^{-5} and 4.00×10^{-5}, respectively, whereas the maximum D_{Li} values at the same temperatures were 2.27×10^{-4}, 3.94×10^{-4} and 6.66×10^{-4}, respectively. Similarly, the minimum D_{Na} values for experiments performed at 25, 15 and 5 °C were 2.38×10^{-5}, 2.60×10^{-5} and 5.71×10^{-5}, respectively, whereas the maximum D_{Na} values at the same temperatures were 1.24×10^{-4}, 1.75×10^{-4} and 2.79×10^{-4}, respectively.

The dependence of D_{Li} on aragonite growth rate as calculated using Eq. (1) for experiments conducted at 25, 15 and 5 °C respectively, can be expressed with the aid of the equations:

$$LogD_{Li,25} = 0.865(\pm 0.049) Log\ r_p + 2.538(\pm 0.380); R^2 = 0.96 \quad (3a)$$

$$LogD_{Li,15} = 0.801(\pm 0.056) Log\ r_p + 2.292(\pm 0.429); R^2 = 0.95 \quad (3b)$$

$$LogD_{Li,5} = 0.840(\pm 0.044) Log\ r_p + 2.867(\pm 0.344); R^2 = 0.97 \quad (3c)$$

Note here that although the absolute values of D_{Li} decrease with increasing temperature, their dependences on growth rate follow similar trends at all temperatures, that is D_{Li} increases as a function of growth rate to a similar extent (Fig. 4A). Similarly, Na incorporation in aragonite at the same geochemical conditions can be described as a function of growth rate with the aid of the equations:

$$LogD_{Na,25} = 0.429(\pm 0.046) Log\ r_p - 0.924(\pm 0.357); R^2 = 0.87 \quad (4a)$$

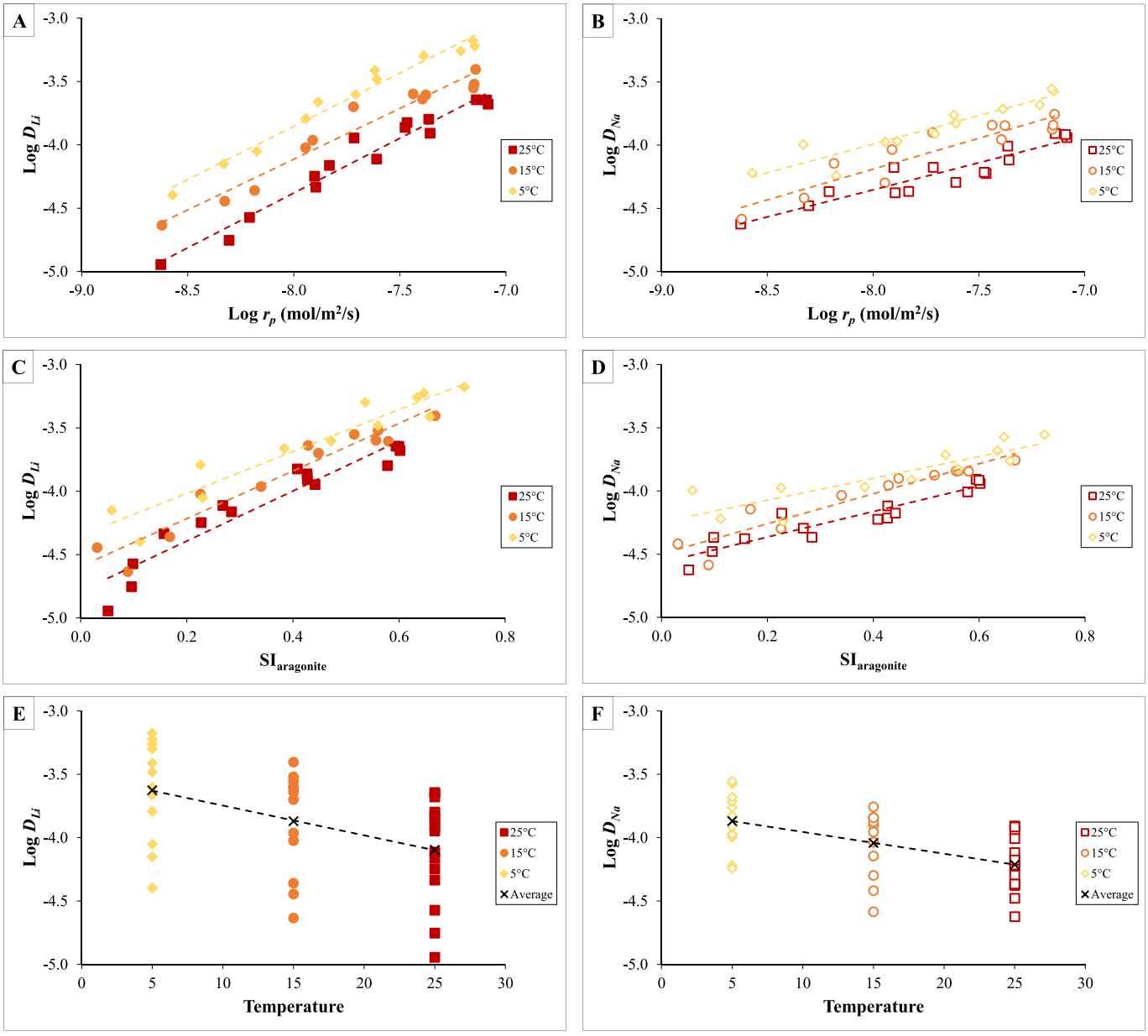

Fig. 4. Dependence of (A) Log D_{Li}, and (B) Log D_{Na} on aragonite growth rate. The associated numerical expressions of the linear trends are described in Eqs. 3a-3c. and 4a-4c. Dependence of (C) Log D_{Li}, and (D) Log D_{Na} on the saturation indices of the reactive solution with respect to aragonite (i.e., $SI_{aragonite}$). The associated numerical expressions of the linear trends are described in Eqs. 7a-7c. and 8a-8c. Dependence of (E) Log D_{Li}, and (F) log D_{Na} on the temperature of the reactive solution during the overgrowth experiments.

$$\mathrm{LogD_{Na,15}} = 0.488(\pm0.063)\mathrm{Log\ r_p} - 0.285(\pm0.488);\ \mathrm{R^2} = 0.86 \quad (4b)$$

$$\mathrm{LogD_{Na,5}} = 0.453(\pm0.052)\mathrm{Log\ r_p} - 0.366(\pm0.402);\ \mathrm{R^2} = 0.88 \quad (4c)$$

These equations are valid for Li and Na under the conditions (i.e., chemical composition of the reactive solutions, temperature, pCO_2, pH) and growth rate ranges investigated in this study; how readily they could be extrapolated to other conditions is not known. The dependence of D_{Li} and D_{Na} on growth rate can be seen in Fig. 4A-B. For both elements a positive correlation is observed between their apparent distribution coefficient in aragonite and growth rate. Furthermore, only small variations in D_{Li} and D_{Na} occur as a function of temperature relative to the changes induced by growth rate (Fig. 4).

Using regression analysis, the effect of both temperature and growth rate on D_{Li} can be described using the equation:

$$Log\ D_{Li} = 0.836(\pm0.028)\ Log\ r_p - 0.026(\pm0.002)\ T + 2.958(\pm0.221);\ R^2 = 0.97 \quad (5)$$

where Log r_p is the growth rate in mol/m^2/s and T is the temperature in °C. Similarly, the effect of temperature and growth rate on D_{Na} values can be described by:

$$Log\ D_{Na} = 0.456(\pm0.030)\ Log\ r_p - 0.018(\pm0.002)\ T - 0.253(\pm0.234);\ R^2 = 0.90 \quad (6)$$

Note here that the use of Eqs. (5) and (6) is valid only for the aragonite growth conditions explored in this study.

4. Discussion

4.1. The effect of growth rate on Me^+ incorporation in aragonite

The results of this study suggest that mineral growth rate strongly affects the incorporation of Me^+ in the solid phase. Indeed, as depicted in Fig. 4A-B, D_{Me^+} values increase up to 1.3 orders of magnitude in the case of Li and up to 0.7 orders of magnitude in the case of Na as growth rate increases from $10^{-8.6}$ to $10^{-7.1}$ (mol/m^2/s) at 25 °C. Similar increases can be observed for experiments conducted at 15 and 5 °C, which exhibit comparable dependencies on growth rate as is evidenced by the identical slopes, within error, of Eqs. 3a-3c and 4a-4c for D_{Li} and D_{Na}, respectively. These results are overall in agreement with those reported earlier by Gabitov et al. (2011) who observed an increase in the Li concentration of aragonite precipitates nucleated from seawater as a function of growth rate.

Previous experimental works have established that mineral growth rate controls the distribution coefficient of trace metals in carbonate minerals (e.g., Lorens, 1981; Tesoriero and Pankow, 1996; Mavromatis et al., 2013). The general behaviour expected for the distribution of trace metals during mineral growth was described by Rimstidt et al. (1998). These authors have shown that the distribution coefficient of Me^{2+} between carbonate minerals and reactive solutions at increasing mineral growth rate tends to unity, that is, the trace to major ratio in the solid approaches that of the solution as growth rate increases. Hence, the thermodynamic considerations that control elemental distribution under near chemical equilibrium conditions do not apply during mineral growth far from equilibrium. Interestingly, although a one-to-one replacement of the trace metal for Ca^{2+} in the crystal lattice may not occur for Me^+, similar effects have been observed during the incorporation of other, incompatible, ions during carbonate mineral growth. For example, the distribution coefficients of REE decrease at increasing calcite growth rate (e.g., Voigt et al., 2017), whereas the distribution of B in calcite and aragonite increases at elevated mineral growth rates (e.g., Gabitov et al., 2014; Mavromatis et al., 2015; Uchikawa et al., 2015, 2017). Based on the correlations of D_{Me^+} with growth rate that can be seen in Fig. 4A-B it is therefore suggested that the model proposed by Rimstidt et al. (1998) can also be used to assess the behaviour of Li and Na during their incorporation in aragonite, and as such the D_{Li} and D_{Na} would approach unity at high enough growth rate. The latter assumption remains however hypothetical because of the probable nucleation or formation of precursors (e.g., ACC) at the growth rate needed for D_{Li} and D_{Na} to theoretically reach unity.

For all the three temperatures investigated, D_{Li} values exhibit an increase of ~1.3 orders of magnitude when growth rate increases ~1.5 orders of magnitude (Table 1; Fig. 4A-B). This magnitude of increase is somewhat lower than that observed during incorporation of Li in calcite, where an increase of ~2 orders of magnitude in $D_{Li,calcite}$ values over an increase of ~1 order of magnitude in mineral growth rate occurs (Füger et al., 2019). While high sensitivities of D_{Me} to mineral growth rate in a particular mineral have been previously documented (e.g., D_{Sr} in calcite or D_{Ni} in aragonite; Tang et al., 2008; Brazier and Mavromatis, 2022), such high sensitivities in both calcite and aragonite of D_{Me^+} values to mineral growth rate have never been reported for other metal cations. For example, Ba exhibits an incompatible behaviour during its incorporation in both calcite and aragonite with D_{Me}^{2+} increasing by 0.35–0.5 orders of magnitude when growth rate increases ~1 order of magnitude (Mavromatis et al., 2018). Additionally, as can be seen in Fig. 4A-B, the incorporation of Na in aragonite exhibits roughly half the sensitivity to growth rate compared to Li in the experimental runs of this study. Indeed, the slope of Eqs. 3a-3c is roughly double that of Eqs. 4a-4c for the same set of experimental runs. It is likely that the greater dependence of D_{Li} compared to D_{Na} on mineral growth rate stems from the mechanism of Li incorporation into aragonite. Indeed, the incorporation of Li and Na in aragonite do not form a solid-solution with aragonite, rather these traces behave as impurities, the incorporation of which in the solid is likely controlled by the presence of surface defects sites. The dependence of D_{Li} and D_{Na} values on reactive solution supersaturation with respect to aragonite supports the presence of such a mechanism (Fig. 4C-D), as surface defect density tends to increase as a function of increasing growth rate and supersaturation (e.g., Busenberg and Plummer, 1985; McDermott et al., 1999; Frisia et al., 2000; Teng et al., 2000; Wynn et al., 2018). Furthermore, two other factors in this study point towards Li and Na attachment in surface defect sites: (i) the inability of Li to increase its coordination to 9 to ideally substitute for Ca (Olsher et al., 1991), and (ii) the charge imbalance that requires compensation. For the three temperatures investigated here, the relationship between D_{Li} or D_{Na} and $SI_{aragonite}$ can be described by the following equations (for information a similar relationship considering an average of all the data is given):

$$LogD_{Li,25} = 1.973(\pm0.173)SI_{aragonite} - 4.788(\pm0.069);\ R^2 = 0.91 \quad (7a)$$

$$\mathrm{LogD_{Li,15}} = 1.879(\pm0.161)\mathrm{SI_{aragonite}} - 4.592(\pm0.070);\ \mathrm{R^2} = 0.93 \quad (7b)$$

$$\mathrm{LogD_{Li,5}} = 1.654(\pm0.170)\mathrm{SI_{aragonite}} - 4.348(\pm0.083);\ \mathrm{R^2} = 0.90 \quad (7c)$$

$$\mathrm{LogD_{Li,average\ T°C}} = 1.937(\pm0.138)\mathrm{SI_{aragonite}} - 4.632(\pm0.061);\ \mathrm{R^2} = 0.84 \quad (7d)$$

$$\mathrm{LogD_{Na,25}} = 1.011(\pm0.105)\mathrm{SI_{aragonite}} - 4.567(\pm0.042);\ \mathrm{R^2} = 0.88 \quad (8a)$$

$$\mathrm{LogD_{Na,15}} = 1.186(\pm0.128)\mathrm{SI_{aragonite}} - 4.497(\pm0.056);\ \mathrm{R^2} = 0.90 \quad (8b)$$

$$\mathrm{LogD_{Na,5}} = 0.862(\pm0.151)\mathrm{SI_{aragonite}} - 4.246(\pm0.074);\ \mathrm{R^2} = 0.77 \quad (8c)$$

$$\mathrm{LogD_{Na,average\ T°C}} = 1.098(\pm0.110)\mathrm{SI_{aragonite}} - 4.480(\pm0.048);\ \mathrm{R^2} = 0.73 \quad (8d)$$

Interestingly, for all the experiments performed in this study D_{Li} values are on average ~ 1.5 times higher than the corresponding D_{Mg}

values reported in Mavromatis et al. (2022), while the D_{Na} values are on average similar to the corresponding D_{Mg} values independent of growth temperature. At present it is unclear why a difference occurs between Li and Mg and not between Na and Mg considering that the ionic radii of Li and Mg are similar, but Na is significantly larger (i.e., Li: 0.76 Å, Mg: 0.72 Å, Na: 1.02 Å in 6-fold coordination; Shannon, 1976). In addition, all three elements are primarily present as free ions (i.e., >99% Li^+, >99% Na^+, 92% Mg^{2+}) in the reactive solution. However, there is a difference in the rate of exchange of water ions between the water molecules in the hydration sphere of the free ion and the bulk water between Mg, Na, and Li (i.e. $\sim 5 \times 10^5$ s^{-1} for Mg, $\sim 6 \times 10^8$ s^{-1} for Li, and 10^9 s^{-1} for Na; Lincoln and Merbach, 1995; Loeffler et al., 2006). If it is assumed that partial or complete dehydration is required for the incorporation of these ions in the solid, the difference in water exchange rates may be an important parameter controlling the presence of these cations in the solid. However, D_{Mg} and D_{Na} values are similar despite Mg and Na exhibiting the largest difference in water molecule exchange rate, and despite more similar water exchange rates for Li and Na, the D_{Li} and D_{Na} differ substantially. These observations suggest that the water exchange rate is probably not the main control over the incorporation rate of Li and Na within aragonite. Another parameter that may explain the different behaviour observed for these three ions is their affinities for the aqueous solution as described by the Gibbs free energy of their hydration in aqueous solution. The hydration energies are far higher for Li^+ and Na^+ than Mg^{2+} (i.e., −475 kJ/mol, −365 kJ/mol and −1830 kJ/mol, respectively; Marcus, 1991). Thus, the differences between D_{Mg}, D_{Na} and D_{Li} are also unlikely related solely to the hydration energy. Another possibility arises from the poor constraints on the mechanisms of altervalent substitution of trace in carbonate minerals. In fact, it is likely that the above-mentioned parameters (i.e., ionic radius and hydration of aqueous ion) affect only partly the incorporation of ions in $CaCO_3$ minerals and thus their distribution coefficient. In contrast, the difference in valence between Mg^{2+} and Li^+ or Na^+ and the necessity for charge compensation during the incorporation of the latter in the $CaCO_3$ structure is likely the process that primarily controls the presence of these elements in the solid, thus making the comparison of distribution coefficients between monovalent and divalent ions extremely difficult. Despite their incompatibility with the aragonite structure, differences in distribution coefficients for these three elements are significant. It is particularly intriguing that the distribution coefficient of Li^+ is higher than Mg^{2+}, despite the charge imbalance implied by its incorporation. Unfortunately, the mechanism of incorporation could not be fully resolved with the available data, but the relatively high incorporation of both Na and Li in the solid, being similar to or higher than incorporation of Mg, suggests these elements may be useful proxies and thus their mechanism of incorporation is worthy of investigation.

Not only was D_{Mg} lower than D_{Li}, but the D_{Na} was, on average, 1.9 times lower than D_{Li} values (Table 1). The lower D_{Na} compared to D_{Li} suggests that the incorporation of Me^+ in aragonite follows a quite similar trend to that of calcite albeit with a difference in absolute values. Indeed, the presence of Li and Na in calcite presented by Füger et al. (2019) is characterized by ~7 times lower D_{Na} values compared to D_{Li} values. However, our results are not in agreement with the results of Okumura and Kitano (1986), who suggested that Na^+ is more easily incorporated than Li^+ in aragonite because of the more similar ionic radius between Na^+ and Ca^{2+} than between Li^+ and Ca^{2+}. The opposite tendency observed in our study suggests that the difference in ionic radius between Li and Na does not impact the presence of these elements in the solid phase if an ion-to-ion replacement for Ca^{2+} is considered. Furthermore, the proximity of D_{Na} and D_{Li} values recorded in this study and by Füger et al. (2019) suggest that the incorporation of both Li and Na is not particularly favoured in aragonite compared to calcite as was proposed by Okumura and Kitano (1986). Yoshimura et al. (2017) argued that Na^+ incorporation in both natural calcite and aragonite is likely the result of an ion-to-ion substitution of Na^+ for Ca^{2+} based on XANES spectroscopic data. These authors, following the model proposed by White (1977), assumed that the charge imbalance imparted by this substitution is likely counterbalanced by the formation of CO_3^{2-} vacancies (i.e., $2Ca^{2+} \rightarrow 2Na^+$ and a CO_3^{2-} vacancy). Based on the close values of D_{Na} and D_{Li} measured in this study it can be argued that a similar substitution mechanism may explain the presence of Li in aragonite.

4.2. Control of temperature on Li and Na incorporation in aragonite

Temperature exerts a minor control on Li and Na incorporation in aragonite compared to the effect of growth rate (Fig. 4E-F). Indeed, D_{Li} values in experiments conducted at 5 °C are on average ~ 1.7 times higher than at 15 °C and 2.9 times higher than at 25 °C for aragonite formed at similar surface normalized growth rates. This increase is significantly lower compared to the overall increase in D_{Li} of ~17 to 20 times measured between the slowest and fastest growth rate (i.e., 1.5 order of magnitude difference) at the three considered temperatures. Similarly, D_{Na} values in experiments conducted at 5 °C are ~1.5 times higher than at 15 °C and 2.2 times higher than at 25 °C for aragonite formed at similar surface normalized growth rates. This increase is also smaller compared to the increase of 5 to 7 times of D_{Na} values between the slowest and fastest growth rate at the three considered temperatures.

Previously, Marriott et al. (2004a) have shown that temperature affects the incorporation of Li in calcite, with a systematic decrease of the apparent $D_{Li,calcite}$ with increasing temperature. Note here, however that these authors did not control growth rate in their experiments which can also vary due to the retrograde solubility of calcite as a function of temperature (i.e., a lower SI at a lower temperature for the same ion activity product), and a resulting change in growth rate. If the incorporation of Li in either calcite or aragonite is indeed associated with the presence of surface defects sites, then it can be expected that a similar behaviour of D_{Li} values as a function of temperature would be met for both $CaCO_3$ polymorphs. The values of $D_{Li,calcite}$ *values* presented by Marriott et al. (2004a) are systematically higher than the one for aragonite of this work but also higher compared to the results presented by Füger et al. (2019) for Li in calcite, the latter being similar to the results of this study. These differences probably stem from the fact that the growth rate of Marriott et al. (2004a) is likely higher than the ones investigated in both this study and the study of Füger et al. (2019). Additionally, the observed differences in D_{Li} may also be attributable to different pH conditions used in the study of Marriott et al. (2004a). As has been shown earlier in Füger et al. (2019) the apparent distribution coefficient of Li in calcite decreases with increasing pH for solids formed under similar surface normalized growth rates. In the present study, aragonite was precipitated at pH ~8.2, similar to calcite in the work by Füger et al. (2019), whereas Marriott et al. (2004a) formed calcite at a pH of 6.9–7.1. Nevertheless, despite the higher $D_{Li,calcite}$ reported by Marriott et al. (2004a) compared to the D_{Li} of this study, the effect of temperature on D_{Li} is in a similar range for both minerals i.e., D_{Li} is 1.7 and 2.7 times higher at 5 °C than at 15 and 25 °C in calcite, respectively, compared to 1.7 and 2.8 times higher at 5 °C than at 15 and 25 °C, respectively, observed for aragonite.

As mentioned previously, at an increasing degree of reactive solution saturation with respect to a $CaCO_3$ phase, the amount of surface defect sites on the growing mineral increases. These defect sites offer a pathway for the incorporation of elements that are incompatible with the crystal structure (e.g., Busenberg and Plummer, 1985). Thus, it seems likely that the incorporation of Li and Na in aragonite is dependent on the amount of defect sites. The growth rate and the saturation state of the solution with respect to aragonite are linearly correlated at low degrees of fluid saturation with respect to aragonite and at constant temperature. Interestingly, by comparing experiments performed at different temperatures, it is possible to decouple the growth rate and the fluid saturation with respect to aragonite. For example, the experiments LiAr-6, LiAr-12 and LiAr-24, performed at 25, 15 and 5 °C, respectively, exhibit similar growth rate (i.e., $10^{-7.5}$ mol/m^2/s) and subsequently

increasing $SI_{aragonite}$ at decreasing temperature (i.e., 0.43, 0.58 and 0.66 at 25, 15 and 5 °C, respectively). These three experiments at similar normalized growth rates however show an increase of D_{Li} and D_{Na} with decreasing temperature, which indicates that the number of defects formed during mineral growth is more likely related to the saturation indices of the solutions with respect to aragonite than to the growth rate.

Although mineral growth rate is the main factor controlling D_{Me^+} values in aragonite in this study, the direct impact of temperature can still be estimated. The effect of temperature is pronounced at low mineral growth rates where aragonite growth occurred at similar $SI_{aragonite}$ in all the three temperatures explored in this study. This is for example the case for experiments LiAr-13, LiAr-7 and LiAr-19, which were performed at $SI_{aragonite}$ of ~0.10, but are characterized by measurably different D_{Li} values increasing from $10^{-4.75}$ at 25 °C to $10^{-4.40}$ at 5 °C. In the same set of samples, D_{Na} also exhibits temperature related variations, obtaining values of $10^{-4.48}$ at 25 °C (LiAr-13) and $10^{-4.22}$ at 5 °C (LiAr-19). The same effect was observed for the D_{Mg} values derived from the same samples presented by Mavromatis et al. (2022). This direct control of the temperature on the incorporation of Li and Na at conditions close to equilibrium remains intriguing. Marriott et al. (2004a) proposed that the incorporation of Li in calcite is exothermic and that incorporation on certain crystal faces is favoured at low temperature. It is likely that a similar process affects the incorporation of Li and Na in aragonite. Nevertheless, the mechanisms controlling the distribution behaviour at low growth rate remain unsolved and need further investigation.

4.3. Mineral growth rate and temperature controls on Li/Mg and Na/Mg ratios in aragonite

The results of this study combined with those presented in Mavromatis et al. (2022), demonstrate that the incorporation of Li, Na and Mg in aragonite is mainly controlled by growth rate, whereas the effect of temperature is significantly smaller. The effect of temperature on D_{Li}, D_{Na} and D_{Mg} can be divided into two categories with the first related to the effect of temperature on solution saturation with respect to

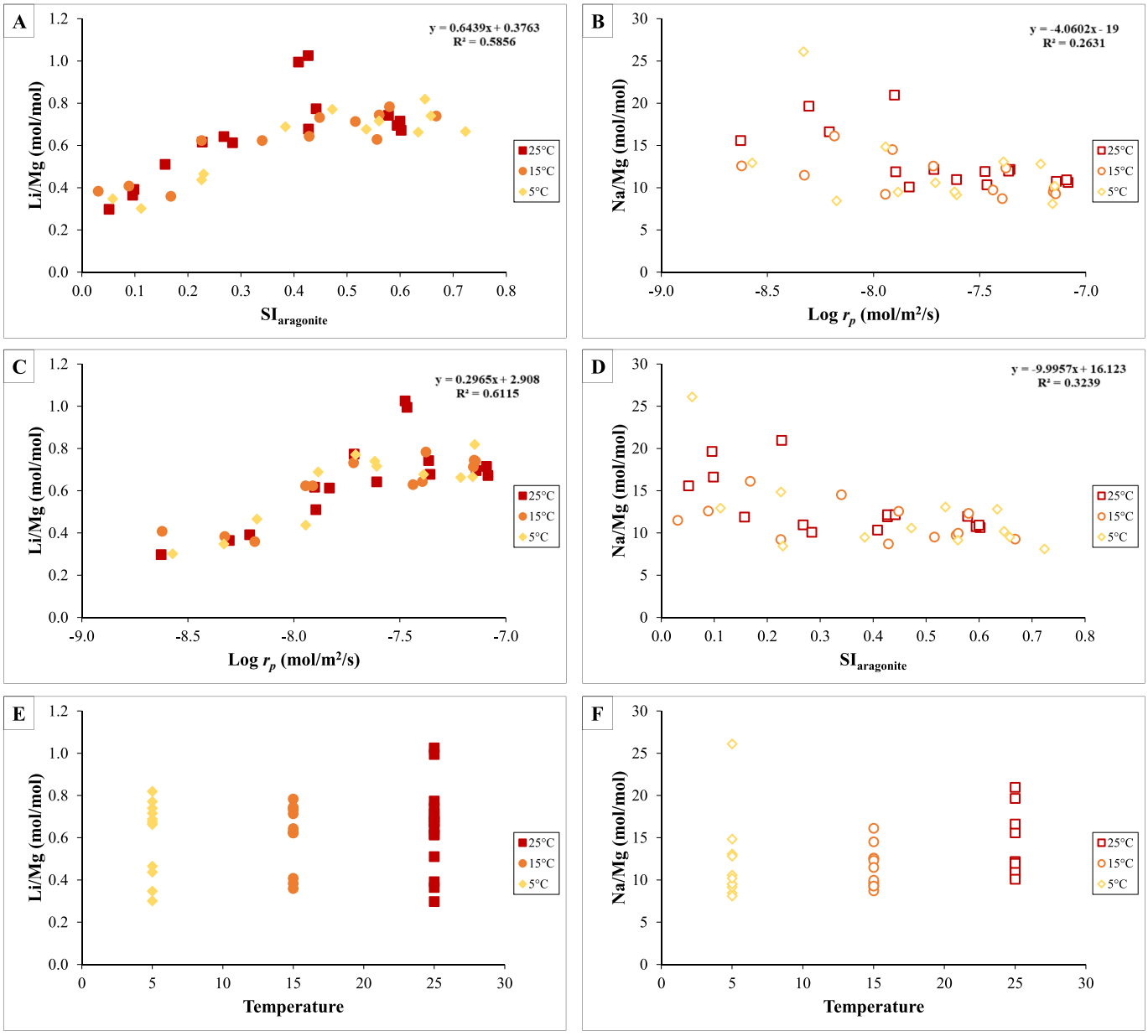

Fig. 5. Dependence of the Li/Mg and Na/Mg ratio of the aragonite overgrowth to the temperature of the reactive solution (A and B, respectively), to the growth rate (C and D, respectively), and to saturation indices of the reactive solution with respect to aragonite (E and F, respectively).

aragonite, and the second to a direct effect of temperature on the incorporation, mainly evident in distribution coefficients at conditions close to thermodynamic equilibrium. While a slight negative correlation exists between Na/Mg and growth rate, a positive correlation exists between the Li/Mg ratio in the precipitated mineral and the growth rate with an increase in the ratio as the growth rate increases (Fig. 5A-B). The same trend can be observed between Na/Mg and Li/Mg and saturation indices of the solution with respect to aragonite (Fig. 5C-D). Yet, as can be seen in Fig. 5E and F, temperature has no significant effect on Na/Mg and Li/Mg, considering the similar range in ratios measured at the three temperatures investigated. These dependencies of Na/Mg and Li/Mg ratio on growth rate and temperature can be described by the following linear equations:

$$\frac{Na}{Mg} = -4.122\ (\pm 1.116)\ Log\ r_p + 0.066\ (\pm 0.062)\ T - 20.523\ (\pm 8.710); R^2 = 0.29 \quad (9)$$

$$\frac{Li}{Mg} = 0.295\ (\pm 0.039)\ Log\ r_p + 0.001\ (\pm 0.002)\ T + 2.879\ (\pm 0.306); R^2 = 0.62 \quad (10)$$

Interestingly, Eq. (8) shows that Na/Mg does not respond to temperature within error, and while correlations between Na/Ca or Mg/Ca and growth rate exist, it seems that Na/Mg does not respond strongly to growth rate. Based on the low correlation between Na/Mg and both growth rate and temperature, this ratio appears to be a poor proxy for these parameters. Nevertheless, based on Eq. (10), growth rate appears to have a significant impact on the Li/Mg ratio although the correlation coefficient (R^2) is lower than in the case of the Li/Ca (see Eqs. 3a-3c) or Mg/Ca ratio (see Mavromatis et al., 2022). This correlation between Li/Mg and growth rate can be explained by the higher dependence of Li incorporation on growth rate than Mg (see Mavromatis et al., 2022). These results are in contrast to those of Gabitov et al. (2011), who showed that during Mg and Li incorporation in aragonite, the dependence of Li on growth rate is lower than that of Mg. The different results between the present study and Gabitov et al. (2011) can be assigned to some extent to the experimental protocols and in particular the use of seawater in the experiments of Gabitov et al. (2011), which may affect differently the elemental incorporation during mineral growth. For example, the presence of SO_4^{2-} in the aqueous medium may promote Mg incorporation in the solid as the Mg-bearing $MgSO_4^0$ (aq) complex, a process which distorts the hydration sphere of Mg^{2+} (aq) and offers a possible incorporation mechanism for Mg in the aragonite structure. In contrast Li occurs primarily as free $Li^+_{(aq)}$ ion in seawater.

It is interesting to note that the Li/Mg ratio of biogenic aragonite has been used as a temperature proxy (e.g., Case et al., 2010; Hathorne et al., 2013; Raddatz et al., 2013; Montagna et al., 2014; Marchitto et al., 2018; Cuny-Guirriec et al., 2019; Stewart et al., 2020), whereas the results of this study show a negligible temperature effect on the Li/Mg ratio in abiotic aragonite. Indeed, the main impact of temperature on Li incorporation in abiotic aragonite seems to be on the degree of solution saturation with respect to aragonite. Numerous studies on natural aragonitic samples, commonly of coralline origin, observed a strong correlation of Li/Mg ratio with temperature. For example, Montagna et al. (2014) showed a strong exponential correlation between Li/Mg and temperature for 38 specimens of corals covering a range of Li/Mg of ~1.2 to 5.2 and a range of temperature of 0.8 to 28 °C. This correlation between Li/Mg and temperature does not exist in the precipitates of this study, which exhibit a similar range of Li/Mg at the three investigated temperatures (i.e., 5, 15 and 25 °C), and an increase of Li/Mg for $SI_{aragonite}$ values between 0.03 and 0.40, and similar Li/Mg values above $SI_{aragonite} = 0.4$. The biological nature of the coral samples and microstructural variations associated with their growth processes may play a role in the difference in temperature dependence of Li/Mg values observed. Previous studies have shown that Li and Mg behave similarly during biomineralization processes and that the use of the Li/Mg ratio in aragonite is independent of saturation effects, calcification, or interspecies variations (e.g., Bryan and Marchitto, 2008; Case et al., 2010; Hathorne et al., 2013; Raddatz et al., 2013; Montagna et al., 2014; Cuny-Guirriec et al., 2019; Stewart et al., 2020). These assumptions, however, have been questioned by other studies which have shown that microstructural biases on Li and Mg incorporation between Thickening Deposits (TDs) and Centers of Calcification (COCs) exist and that significant differences in Li/Ca and Mg/Ca can be observed depending on the coral growth environment (e.g., Rollion-Bard and Blamart, 2015; Fowell et al., 2016). For example, Rollion-Bard and Blamart (2015) proposed that kinetic effects, and thus the number of defect sites linked to the growth rates, played a significant role in the incorporation of Li and Mg in coral skeletons. According to their study, temperature plays only an indirect role, particularly when biological processes impact the growth rate. In contrast, Fowell et al. (2016) highlighted a poor correlation between sea surface temperature and the Li/Mg ratio in backreef corals compared to the ratio of forereef corals. This seems also to indicate that not only temperature but also other parameters affect the Li/Mg ratio in natural aragonite.

The absence of correlation between Li/Mg and temperature in this study compared to natural biogenic aragonite could also arise from the experimental design that is different to aragonite growth in natural environments and specifically during biomineralization processes. Indeed, in the experimental setup used in this study, growth occurs at chemical steady-state conditions due to the continuous supply of elements in the reactive solution, making the reservoir infinite with respect to Li and Mg. During biomineralization, aragonite growth is often controlled by mechanisms occurring in limited reservoirs, notably Rayleigh fractionation (e.g., corals), which does not occur in the abiotic growth experiment setup. Note also that in general, $\Omega_{aragonite}$ in this study is close to thermodynamic equilibrium and lower than those typically occurring during biomineralization (i.e., $\Omega > 10$, DeCarlo et al., 2017; Farfan et al., 2018). Thus, while the results of this study on abiotic aragonite grown in a controlled environment agree with the conclusions of Rollion-Bard and Blamart (2015), it remains difficult to extrapolate them to natural biotic samples. Nevertheless, these findings highlight the importance of an abiotic baseline to provide valuable insight into mechanisms related to incorporation of traces into biogenic aragonite.

4.4. Mechanisms of Me^+ incorporation in aragonite

The understanding of the parameters controlling Li and Mg incorporation in abiotic aragonite remains currently limited. Nevertheless, the mechanisms controlling the Li/Mg ratio in abiotic aragonite do not seem to be controlled by a single parameter. Indeed, the results of this study together with those of Mavromatis et al. (2022) for Mg in aragonite, show a clear effect of the mineral growth rate on Li, Na and Mg incorporation. However, it is difficult to extrapolate these results to natural marine environments, in particular due to the absence of certain ions (e.g., SO_4) known to affect the incorporation of trace elements into carbonate minerals by alteration of the mineral structure (e.g., Mucci and Morse, 1983; Busenberg and Plummer, 1985; Goetschl et al., 2019). Beyond these limitations, it seems that D_{Li} and D_{Na} in aragonite are robust tracers of growth rate, within a multi-proxy approach context, that requires temperature estimation using another geochemical tool. The main outcome of this is the weak effect of temperature on D_{Li}, which can also be extended to the Li/Mg ratio in abiotic aragonite. These results are nevertheless surprising in light of previous studies supporting the use of Li/Mg in coralline aragonite as a seawater temperature proxy. If biological effects influencing biomineralization processes can be invoked, it appears that further studies are needed to address the differences between experimental results on abiotic aragonite and natural biogenic aragonite. Understanding the mechanism of trace element

incorporation in both abiotic and biogenic carbonates is essential to their use as paleo-proxies.

Beyond the parameters and processes regulating the incorporation of Li into aragonite in the natural environment, it is interesting to note that the experimental results suggest a strong correlation between D_{Li} and D_{Na} in the precipitated aragonite (Fig. 6A) that can be described through the equation:

$$\mathrm{Log}D_{Li} = 1.543\ (\pm 0.092) \times \mathrm{Log}\ D_{Na} + 2.373\ (\pm 0.374);\ R^2 = 0.88 \quad (11)$$

Interestingly, strong correlations can also be found between D_{Li} and D_{Mg}, and D_{Na} and D_{Mg}, (Fig. 6B-C) described through the equations:

$$\mathrm{Log}D_{Li} = 1.196\ (\pm 0.056) \times \mathrm{Log}\ D_{Mg} + 0.956\ (\pm 0.226);\ R^2 = 0.93 \quad (12)$$

$$\mathrm{Log}D_{Na} = 0.732\ (\pm 0.032) \times \mathrm{Log}\ D_{Mg} - 1.096\ (\pm 0.131);\ R^2 = 0.93 \quad (13)$$

Although the dependencies of Na, Li and Mg on growth rate are different, the correlations between these three ions imply similar incorporation mechanisms in abiotic aragonite. Notably, this good correlation between Li and Na is also present in scleractinian corals (Rollion-Bard and Blamart, 2015) and in high-Mg octocorallian corals (Rollion-Bard et al., 2017). These two studies also invoked a similar incorporation mechanism between these two monovalent ions.

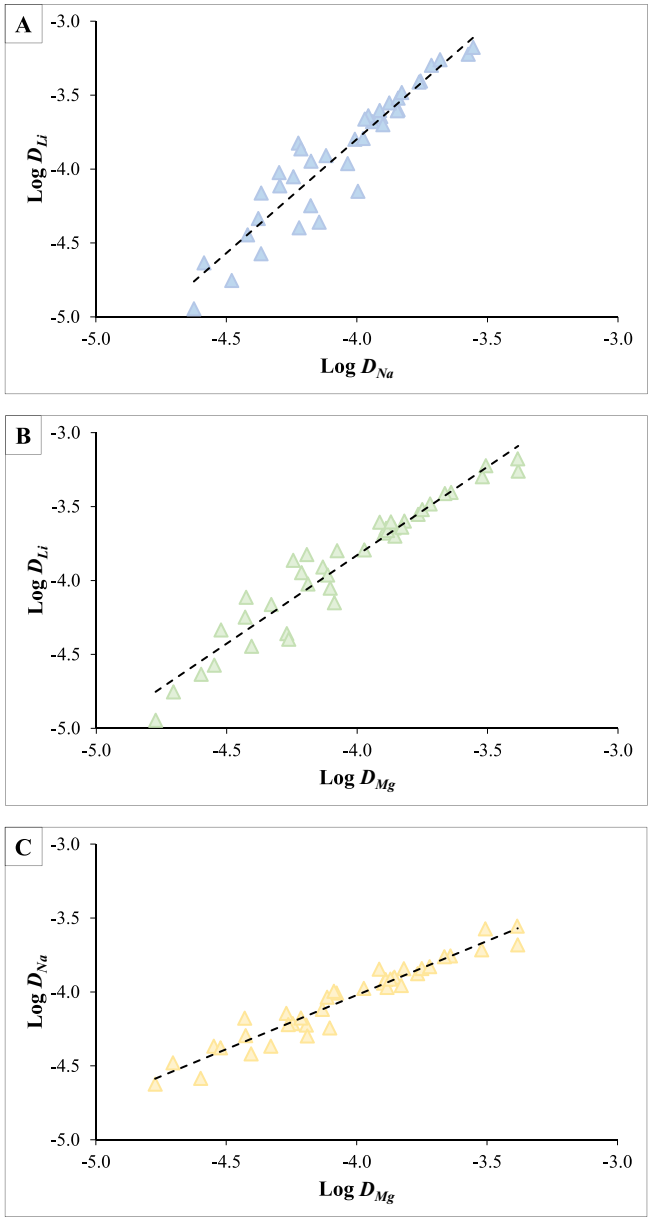

Fig. 6. Relationship of (A) Log D_{Li} on Log D_{Na}, (B) Log D_{Li} on Log D_{Mg}, and (C) Log D_{Na} on Log D_{Mg}. The numerical expressions of the linear trends are described in Eq. 11, 12, and 13, respectively.

It appears likely that the mechanism driving the presence of these three elements in aragonite is their incorporation at mineral defect sites, where the crystallographic structures are disordered. Indeed, although an altervalent substitution of Ca^{2+} with Na^{+}, coupled with CO_3^{2-} vacancies to compensate for the charge deficit, has been proposed by Yoshimura et al. (2017), it is difficult to imagine that Li^{+} and Mg^{2+} would follow the same pathway of incorporation due to their small ionic radii, which hinders development of 9-fold coordination in the solid. Further studies on the bonding environment within the crystal lattice are necessary to address precisely these questions of the difference between D_{Li} and D_{Na} recorded in this study. Aside from mechanistic considerations, the intercorrelations between D_{Li}, D_{Na}, *and* D_{Mg} as expressed using Eqs. (12) and (13) suggest that the Li^{+}, Na^{+}, and Mg^{2+}concentrations in the solution could be approximated if at least one of the three concentrations in the solid is known or can be reasonably estimated. It has to be noted that the application of these correlations is valid for abiotically precipitated aragonite in the physicochemical condition of this work. Considering the difference in fluid composition between this work and natural seawater (i.e., the fluid composition can affect the incorporation process, e.g., Gabitov et al., 2019) and the numerous biological effects that could overprint the abiotic control on ion distribution, the application to natural seawater environments has to be considered with great caution.

5. Conclusions

The results of this study show that Li and Na are incorporated in small amounts during aragonite growth following the classical behaviour of elements incompatible with the host mineral structure. Mechanistically, the incorporation of Li and Na in aragonite is probably related to the amount of defect sites on the mineral surface, which is known to increase when the saturation state of the fluid and the growth rate increase. These results indicate that the distribution coefficient of both Na and Li in aragonite can be used as a proxy for mineral growth rate. The similar behaviour observed between Li, Na, and Mg distribution coefficients in aragonite suggests a similar mechanism of incorporation. This mechanism and the position of such monovalent ions in the crystal structure (i.e., direct substitution with Ca^{2+} or interstitial incorporation) is however still under debate as it is difficult to reconcile the highly different physiochemical parameters (e.g., ionic radii, valence, energy of hydration) of these three elements around a common driving mechanism. Additional data are needed to describe their bonding environments within aragonite the crystal lattice. Interestingly, the strong intercorrelation between D_{Li}, D_{Na}, and D_{Mg} indicates that one of these distribution coefficients can be used to approximate the other two and as such the trace element concentration in the reactive solution from which the mineral was formed in the studied system.

The main outcome of this work is that temperature has a negligible effect on the D_{Li} and D_{Na} distribution coefficients in abiotically precipitated aragonite. The fluid temperature seems to exhibit two effects on Li and Na incorporation, (1) an indirect effect on the saturation state of the reactive solution promoting a higher number of defect sites at lower temperature, (2) a direct effect on the incorporation at conditions close to equilibrium, which remains unclear. In both cases, these temperature effects are rather small compared to the effect of the mineral growth rate on Na and Li incorporation. Interestingly, a similar observation was made for the Li/Mg ratio of the precipitated aragonite, with a much stronger control of the growth rate compared to temperature. These results contrast with the observed temperature dependence of Li/Mg ratio in aragonitic corals as a seawater temperature proxy. It is therefore important to continue experimental work as a baseline to address the

observed discrepancy between the elemental ratio in abiotically precipitated and biogenic aragonite and the parameters controlling them to allow for robust proxy development and interpretation of trace elements in natural carbonate archives.

CRediT authorship contribution statement

Jean-Michel Brazier: Writing – review & editing, Writing – original draft, Validation, Methodology, Investigation, Formal analysis, Data curation, Conceptualization. **Anna L. Harrison:** Writing – original draft, Writing – review & editing. **Claire Rollion-Bard:** Writing – original draft, Writing – review & editing. **Vasileios Mavromatis:** Writing – original draft, Methodology, Investigation, Funding acquisition, Data curation, Conceptualization, Writing – review & editing.

Declaration of competing interest

The authors declare the following financial interests/personal relationships which may be considered as potential competing interests:

Jean-Michel Brazier reports financial support was provided by Austrian Science Fund. Vasileios Mavromatis reports financial support was provided by National Centre for Scientific Research. If there are other authors, they declare that they have no known competing financial interests or personal relationships that could have appeared to influence the work reported in this paper.

Data availability

Data will be made available on request.

Acknowledgments

We thank Andrea Wolf and Maria Hierz for their technical support. For assistance with SEM analyses, the authors are thankful to Gerald Auer. Katja Goetschl is particularly acknowledged for her support in the lab and for the fruitful discussion, and assistance with XRD. This work was funded by the French National program INSU/LEFE, and the FWF project P31832-N29.

Appendix A. Supplementary data

Supplementary data to this article can be found online at https://doi.org/10.1016/j.chemgeo.2024.122057.

References

Brazier, J.-M., Mavromatis, V., 2022. Effect of growth rate on nickel and cobalt incorporation in aragonite. Chem. Geol. 600, 120863.
Bonneau, L., Colin, C., Pons-Branchu, E., Mienis, F., Tisnérat-Laborde, N., Blamart, D., Elliot, M., Collart, T., Frank, N., Foliot, L., Douville, E., 2018. Imprint of Holocene Climate Variability on Cold-Water Coral Reef Growth at the SW Rockall Trough Margin, NE Atlantic. Geochem. Geophys. Geosyst. 19 (8), 2437–2452.
Brazier, J.-M., Blanchard, M., Méheut, M., Schmitt, A.-D., Schott, J., Mavromatis, V., 2023. Experimental and theoretical investigations of stable Sr isotope fractionation during its incorporation in aragonite. Geochim. Cosmochim. Acta 358, 134–147.
Brunauer, S., Emmett, P.H., Teller, E., 1938. Adsorption of gases in multimolecular layers. J. Am. Chem. Soc. 60 (2), 309–319.
Bryan, S.P., Marchitto, T.M., 2008. Mg/Ca–temperature proxy in benthic foraminifera: New calibrations from the Florida Straits and a hypothesis regarding Mg/Li. Paleoceanography 23 (2).
Burton, W.K., Cabrera, N., Frank, F.C., 1951. The growth of crystals and the equilibrium structure of their surfaces. Philosophical Transactions of the Royal Society of London. Series A. Math. Phys. Sci. 243 (866), 299–358.
Busenberg, E., Plummer, L.N., 1985. Kinetic and thermodynamic factors controlling the distribution of SO_3^{2-} and Na^+ in calcites and selected aragonites. Geochim. Cosmochim. Acta 49 (3), 713–725.
Case, D.H., Robinson, L.F., Auro, M.E., Gagnon, A.C., 2010. Environmental and biological controls on Mg and Li in deep-sea scleractinian corals. Earth Planet. Sci. Lett. 300 (3–4), 215–225.
Cuny-Guirriec, K., Douville, E., Reynaud, S., Allemand, D., Bordier, L., Canesi, M., et al., 2019. Coral Li/Mg thermometry: caveats and constraints. Chem. Geol. 523, 162–178.
DeCarlo, T.M., D'Olivo, J.P., Foster, T., Holcomb, M., Becker, T., McCulloch, M.T., 2017. Coral calcifying fluid aragonite saturation states derived from Raman spectroscopy. Biogeosciences 14 (22), 5253–5269.
Dromgoole, E.L., Walter, L.M., 1990. Iron and manganese incorporation into calcite: Effects of growth kinetics, temperature and solution chemistry. Chem. Geol. 81 (4), 311–336.
Farfan, G.A., Cordes, E.E., Waller, R.G., DeCarlo, T.M., Hansel, C.M., 2018. Mineralogy of deep-sea coral aragonites as a function of aragonite saturation state. Front. Marine Sci. 5, 473.
Finch, A.A., Allison, N., 2007. Coordination of Sr and Mg in calcite and aragonite. Mineral. Mag. 71 (5), 539–552.
Finch, A.A., Allison, N., 2008. Mg structural state in coral aragonite and implications for the paleoenvironmental proxy. Geophys. Res. Lett. 35 (8).
Finch, A.A., Allison, N., Steaggles, H., Wood, C.V., Mosselmans, J.F.W., 2010. Ba XAFS in Ba-rich standard minerals and the potential for determining Ba structural state in calcium carbonate. Chem. Geol. 270 (1–4), 179–185.
Fowell, S.E., Sandford, K., Stewart, J.A., Castillo, K.D., Ries, J.B., Foster, G.L., 2016. Intrareef variations in Li/Mg and Sr/ca sea surface temperature proxies in the Caribbean reef-building coral Siderastrea siderea. Paleoceanography 31 (10), 1315–1329.
Frisia, S., Borsato, A., Fairchild, I.J., McDermott, F., 2000. Calcite fabrics, growth mechanisms, and environments of formation in speleothems from the Italian Alps and southwestern Ireland. J. Sediment. Res. 70 (5), 1183–1196.
Füger, A., Konrad, F., Leis, A., Dietzel, M., Mavromatis, V., 2019. Effect of growth rate and pH on lithium incorporation in calcite. Geochim. Cosmochim. Acta 248, 14–24.
Füger, A., Kuessner, M., Rollion-Bard, C., Leis, A., Magna, T., Dietzel, M., Mavromatis, V., 2022. Effect of growth rate and pH on Li isotope fractionation during its incorporation in calcite. Geochim. Cosmochim. Acta 323, 276–290.
Gabitov, R.I., Watson, E.B., 2006. Partitioning of strontium between calcite and fluid. Geochem. Geophys. Geosyst. 7 (11).
Gabitov, R.I., Gaetani, G.A., Watson, E.B., Cohen, A.L., Ehrlich, H.L., 2008. Experimental determination of growth rate effect on U^{6+} and Mg^{2+} partitioning between aragonite and fluid at elevated U^{6+} concentration. Geochim. Cosmochim. Acta 72 (16), 4058–4068.
Gabitov, R.I., Schmitt, A.K., Rosner, M., McKeegan, K.D., Gaetani, G.A., Cohen, A.L., Watson, E.B., Harrison, T.M., 2011. In situ δ^7Li, Li/Ca, and Mg/ca analyses of synthetic aragonites. Geochem. Geophys. Geosyst. 12 (3).
Gabitov, R.I., Rollion-Bard, C., Tripati, A., Sadekov, A., 2014. In situ study of boron partitioning between calcite and fluid at different crystal growth rates. Geochim. Cosmochim. Acta 137, 81–92.
Gabitov, R., Sadekov, A., Yapaskurt, V., Borrelli, C., Bychkov, A., Sabourin, K., Perez-Huerta, A., 2019. Elemental uptake by calcite slowly grown from seawater solution: an in-situ study via depth profiling. Front. Earth Sci. 7, 51.
Gabitov, R.I., Sadekov, A., Dyer, J., Perez-Huerta, A., Xu, H., Migdisov, A., 2021. Sectoral and growth rate control on elemental uptake by individual calcite crystals. Chem. Geol. 585, 120589.
Gaetani, G.A., Cohen, A.L., 2006. Element partitioning during precipitation of aragonite from seawater: a framework for understanding paleoproxies. Geochim. Cosmochim. Acta 70 (18), 4617–4634.
Gautier, Q., Bénézeth, P., Mavromatis, V., Schott, J., 2014. Hydromagnesite solubility product and growth kinetics in aqueous solution from 25 to 75°C. Geochim. Cosmochim. Acta 138, 1–20.
Goetschl, K.E., Purgstaller, B., Dietzel, M., Mavromatis, V., 2019. Effect of sulfate on magnesium incorporation in low-magnesium calcite. Geochim. Cosmochim. Acta 265, 505–519.
Hall, J.M., Chan, L.H., 2004. Li/ca in multiple species of benthic and planktonic foraminifera: Thermocline, latitudinal, and glacial-interglacial variation. Geochim. Cosmochim. Acta 68 (3), 529–545.
Harrison, A.L., Mavromatis, V., Oelkers, E.H., Bénézeth, P., 2019. Solubility of the hydrated Mg-carbonates nesquehonite and dypingite from 5 to 35°C: Implications for CO_2 storage and the relative stability of Mg-carbonates. Chem. Geol. 504, 123–135.
Hathorne, E.C., Felis, T., Suzuki, A., Kawahata, H., Cabioch, G., 2013. Lithium in the aragonite skeletons of massive Porites corals: a new tool to reconstruct tropical sea surface temperatures. Paleoceanography 28 (1), 143–152.
Henderson, L.M., Kracek, F.C., 1927. The fractional precipitation of barium and radium chromates. J. Am. Chem. Soc. 49 (3), 738–749.
Ishikawa, M., Ichikuni, M., 1984. Uptake of sodium and potassium by calcite. Chem. Geol. 42 (1–4), 137–146.
Lakshtanov, L.Z., Stipp, S.L.S., 2004. Experimental study of europium (III) coprecipitation with calcite. Geochim. Cosmochim. Acta 68 (4), 819–827.
Lakshtanov, L.Z., Stipp, S.L.S., 2007. Experimental study of nickel (II) interaction with calcite: Adsorption and coprecipitation. Geochim. Cosmochim. Acta 71 (15), 3686–3697.
Lear, C.H., Rosenthal, Y., 2006. Benthic foraminiferal Li/Ca: Insights into Cenozoic seawater carbonate saturation state. Geology 34 (11), 985–988.
Lear, C.H., Mawbey, E.M., Rosenthal, Y., 2010. Cenozoic benthic foraminiferal Mg/Ca and Li/ca records: toward unlocking temperatures and saturation states. Paleoceanography 25 (4).
Lincoln, S.F., Merbach, A.E., 1995. Substitution reactions of solvated metal ions. Adv. Inorg. Chem. 42 (ARTICLE), 1–88.
Loeffler, H.H., Inada, Y., Funahashi, S., 2006. Water exchange dynamics of lithium (I) ion in aqueous solution. J. Phys. Chem. B 110 (11), 5690–5696.
Lorens, R.B., 1981. Sr, Cd, Mn and Co distribution coefficients in calcite as a function of calcite precipitation rate. Geochim. Cosmochim. Acta 45 (4), 553–561.

Marchitto, T.M., Bryan, S.P., Doss, W., McCulloch, M.T., Montagna, P., 2018. A simple biomineralization model to explain Li, Mg, and Sr incorporation into aragonitic foraminifera and corals. Earth Planet. Sci. Lett. 481, 20–29.
Marcus, Y., 1991. Thermodynamics of solvation of ions. Part 5.—Gibbs free energy of hydration at 298.15 K. J. Chem. Soc. Faraday Trans. 87 (18), 2995–2999.
Marriott, C.S., Henderson, G.M., Belshaw, N.S., Tudhope, A.W., 2004a. Temperature dependence of δ^7Li, δ^{44}Ca and Li/Ca during growth of calcium carbonate. Earth Planet. Sci. Lett. 222 (2), 615–624.
Marriott, C.S., Henderson, G.M., Crompton, R., Staubwasser, M., Shaw, S., 2004b. Effect of mineralogy, salinity, and temperature on Li/ca and Li isotope composition of calcium carbonate. Chem. Geol. 212 (1–2), 5–15.
Mavromatis, V., Gautier, Q., Bosc, O., Schott, J., 2013. Kinetics of Mg partition and Mg stable isotope fractionation during its incorporation in calcite. Geochim. Cosmochim. Acta 114, 188–203.
Mavromatis, V., Montouillout, V., Noireaux, J., Gaillardet, J., Schott, J., 2015. Characterization of boron incorporation and speciation in calcite and aragonite from co-precipitation experiments under controlled pH, temperature and precipitation rate. Geochim. Cosmochim. Acta 150, 299–313.
Mavromatis, V., Immenhauser, A., Buhl, D., Purgstaller, B., Baldermann, A., Dietzel, M., 2017. Effect of organic ligands on Mg partitioning and Mg isotope fractionation during low-temperature precipitation of calcite in the absence of growth rate effects. Geochim. Cosmochim. Acta 207, 139–153.
Mavromatis, V., Goetschl, K.E., Grengg, C., Konrad, F., Purgstaller, B., Dietzel, M., 2018. Barium partitioning in calcite and aragonite as a function of growth rate. Geochim. Cosmochim. Acta 237, 65–78.
Mavromatis, V., Brazier, J.M., Goetschl, K.E., 2022. Controls of temperature and mineral growth rate on Mg incorporation in aragonite. Geochim. Cosmochim. Acta 317, 53–64.
McDermott, F., Frisia, S., Huang, Y., Longinelli, A., Spiro, B., Heaton, T.H., Hawkesworth, C.J., Borsato, A., Keppens, E., Fairchild, I.J., van der Borg, K., Verheyden, S., Selmo, E., 1999. Holocene climate variability in Europe: evidence from δ18O, textural and extension-rate variations in three speleothems. Quat. Sci. Rev. 18 (8–9), 1021–1038.
Montagna, P., McCulloch, M., Douville, E., Correa, M.L., Trotter, J., Rodolfo-Metalpa, R., Dissard, D., Ferrier-Pagès, C., Frank, N., Freiwald, A., Goldstein, S., Mazzoli, C., Reynaud, S., Rüggeberg, A., Russo, S., Taviani, M., 2014. Li/Mg systematics in scleractinian corals: Calibration of the thermometer. Geochim. Cosmochim. Acta 132, 288–310.
Montero-Serrano, J.C., Frank, N., Tisnerat-Laborde, N., Colin, C., Wu, C.C., Lin, K., Shen, C.C., Copard, K., Orejas, C., Gori, A., De Mol, L., Van Rooij, D., Reverdin, G., Douville, E., 2013. Decadal changes in the mid-depth water mass dynamic of the Northeastern Atlantic margin (Bay of Biscay). Earth Planet. Sci. Lett. 364, 134–144.
Morse, J.W., Bender, M.L., 1990. Partition coefficients in calcite: Examination of factors influencing the validity of experimental results and their application to natural systems. Chem. Geol. 82, 265–277.
Mucci, A., Morse, J.W., 1983. The incorporation of Mg^{2+} and Sr^{2+} into calcite overgrowths: influences of growth rate and solution composition. Geochim. Cosmochim. Acta 47 (2), 217–233.
Okumura, M., Kitano, Y., 1986. Coprecipitation of alkali metal ions with calcium carbonate. Geochim. Cosmochim. Acta 50 (1), 49–58.
Olsher, U., Izatt, R.M., Bradshaw, J.S., Dalley, N.K., 1991. Coordination chemistry of lithium ion: a crystal and molecular structure review. Chem. Rev. 91 (2), 137–164.
Paquette, J., Reeder, R.J., 1995. Relationship between surface structure, growth mechanism, and trace element incorporation in calcite. Geochim. Cosmochim. Acta 59 (4), 735–749.
Parkhurst, D.L., Appelo, C.A.J., 2013. Description of Input and Examples for PHREEQC Version 3: A Computer Program for Speciation, Batch-Reaction, One-Dimensional Transport, and Inverse Geochemical Calculations, vols. No. 6-A43. US Geological Survey.
Raddatz, J., Liebetrau, V., Rüggeberg, A., Hathorne, E., Krabbenhöft, A., Eisenhauer, A., Dullo, W.C., 2013. Stable Sr-isotope, Sr/Ca, Mg/Ca, Li/Ca and Mg/Li ratios in the scleractinian cold-water coral lophelia pertusa. Chem. Geol. 352, 143–152.
Reeder, R.J., Lamble, G.M., Northrup, P.A., 1999. XAFS study of the coordination and local relaxation around Co^{2+}, Zn^{2+}, Pb^{2+}, and Ba^{2+} trace elements in calcite. Am. Mineral. 84 (7–8), 1049–1060.
Rimstidt, J.D., Balog, A., Webb, J., 1998. Distribution of trace elements between carbonate minerals and aqueous solutions. Geochim. Cosmochim. Acta 62 (11), 1851–1863.
Rollion-Bard, C., Blamart, D., 2015. Possible controls on Li, Na, and Mg incorporation into aragonite coral skeletons. Chem. Geol. 396, 98–111.
Rollion-Bard, C., Cuif, J.P., Blamart, D., 2017. Optical observations and geochemical data in deep-sea hexa-and octo-coralla specimens. Minerals 7 (9), 154.
Shannon, R.D., 1976. Revised effective ionic radii and systematic studies of interatomic distances in halides and chalcogenides. Acta Crystallogr. Sect. A: Cryst. Phys., Diffr., Theor. Gen. Crystallogr. 32 (5), 751–767.
Stewart, J.A., Robinson, L.F., Day, R.D., Strawson, I., Burke, A., Rae, J.W., et al., 2020. Refining trace metal temperature proxies in cold-water scleractinian and stylasterid corals. Earth Planet. Sci. Lett. 545, 116412.
Tang, J., Köhler, S.J., Dietzel, M., 2008. Sr^{2+}/Ca^{2+} and $^{44}Ca/^{40}Ca$ fractionation during inorganic calcite formation: I. Sr incorporation. Geochim. Cosmochim. Acta 72 (15), 3718–3732.
Temmam, M., Paquette, J., Vali, H., 2000. Mn and Zn incorporation into calcite as a function of chloride aqueous concentration. Geochim. Cosmochim. Acta 64 (14), 2417–2430.
Teng, H.H., Dove, P.M., De Yoreo, J.J., 2000. Kinetics of calcite growth: surface processes and relationships to macroscopic rate laws. Geochim. Cosmochim. Acta 64 (13), 2255–2266.
Tesoriero, A.J., Pankow, J.F., 1996. Solid solution partitioning of Sr^{2+}, Ba^{2+}, and Cd^{2+} to calcite. Geochim. Cosmochim. Acta 60 (6), 1053–1063.
Uchikawa, J., Penman, D.E., Zachos, J.C., Zeebe, R.E., 2015. Experimental evidence for kinetic effects on B/ca in synthetic calcite: implications for potential $B(OH)_4^-$ and $B(OH)_3$ incorporation. Geochim. Cosmochim. Acta 150, 171–191.
Uchikawa, J., Harper, D.T., Penman, D.E., Zachos, J.C., Zeebe, R.E., 2017. Influence of solution chemistry on the boron content in inorganic calcite grown in artificial seawater. Geochim. Cosmochim. Acta 218, 291–307.
Voigt, M., Mavromatis, V., Oelkers, E.H., 2017. The experimental determination of REE partition coefficients in the water-calcite system. Chem. Geol. 462, 30–43.
White, A.F., 1977. Sodium and potassium coprecipitation in aragonite. Geochim. Cosmochim. Acta 41 (5), 613–625.
Wit, J.C., De Nooijer, L.J., Wolthers, M., Reichart, G.J., 2013. A novel salinity proxy based on Na incorporation into foraminiferal calcite. Biogeosciences 10 (10), 6375–6387.
Wynn, P.M., Fairchild, I.J., Borsato, A., Spötl, C., Hartland, A., Baker, A., Frisia, S., Baldini, J.U., 2018. Sulphate partitioning into calcite: Experimental verification of pH control and application to seasonality in speleothems. Geochim. Cosmochim. Acta 226, 69–83.
Yoshimura, T., Tamenori, Y., Suzuki, A., Kawahata, H., Iwasaki, N., Hasegawa, H., Nguyen, L.T., Kuroyanagi, A., Yamazaki, T., Kuroda, J., Ohkouchi, N., 2017. Altervalent substitution of sodium for calcium in biogenic calcite and aragonite. Geochim. Cosmochim. Acta 202, 21–38.
Zhong, S., Mucci, A., 1995. Partitioning of rare earth elements (REEs) between calcite and seawater solutions at 25°C and 1 atm, and high dissolved REE concentrations. Geochim. Cosmochim. Acta 59 (3), 443–453.